

## Article

# Helicoid Morphology of *Arthrospira platensis* NIES-39 Confers Temperature Compensation in the Longitudinal Movement Velocity of Its Trichomes

Hideaki Shiraishi \* , Mari Sasase and Ayano Sakaida Nakashima

Graduate School of Biostudies, Kyoto University, Kyoto 606-8501, Japan; sssmari.uni@gmail.com (M.S.)

\* Correspondence: shiraishi.hideaki.8e@kyoto-u.ac.jp

**Abstract:** The velocity of the gliding movement of filamentous cyanobacteria on a solid surface usually has a strong temperature dependency, and the higher the temperature, the faster the speed. Former studies on this phenomenon were conducted using filamentous cyanobacteria with straight morphology. We examined the velocity of the gliding movement of *Arthrospira platensis* NIES-39 along its longitudinal axis to see if the same was true for this cyanobacterium with helicoid trichomes. Experimental results showed little temperature dependency in the velocity in a wide temperature range in this cyanobacterium. However, when we examined the velocity using mutants with straight trichomes, their velocity was strongly affected by temperature, like other formerly analyzed filamentous cyanobacteria. This result indicates that the helicoid morphology of *A. platensis* trichomes confers temperature compensation to their migration velocity, enabling them to keep a relatively constant velocity under various temperatures. Migration of wild-type trichomes is considerably suppressed compared to the straight-trichome mutants on solid media. The temperature compensation in the locomotion of this organism appears to be established as part of such a suppression. It was also found that the velocity of this cyanobacterium depended on the trichome length when they were atypically short (<250  $\mu\text{m}$ ); the shorter the trichomes, the slower the gliding movement tended to be. This result indicates that the coordinated action of a high number of cells constituting the trichome is required for efficient gliding movement.

**Keywords:** *Arthrospira platensis*; cell movement; cyanobacteria; gliding motility; helix; multicellularity; spirulina; temperature compensation



**Citation:** Shiraishi, H.; Sasase, M.; Nakashima, A.S. Helicoid Morphology of *Arthrospira platensis* NIES-39 Confers Temperature Compensation in the Longitudinal Movement Velocity of Its Trichomes. *Phycology* **2024**, *4*, 104–116. <https://doi.org/10.3390/phycology4010006>

Academic Editor: Assaf Sukenik

Received: 22 November 2023

Revised: 31 January 2024

Accepted: 1 February 2024

Published: 3 February 2024



**Copyright:** © 2024 by the authors. Licensee MDPI, Basel, Switzerland. This article is an open access article distributed under the terms and conditions of the Creative Commons Attribution (CC BY) license (<https://creativecommons.org/licenses/by/4.0/>).

## 1. Introduction

Many filamentous cyanobacteria exhibit gliding motility on solid surfaces [1]. In the early 20th century, researchers analyzed the effect of temperature on the velocity of the gliding movement of various filamentous bacteria (for review, see [2]). They found that the velocity increased in response to an increase in temperature until extremely high temperatures impaired the movement. Since the rate of physical and chemical reactions is generally dependent on temperature, it is natural that the rate of biological processes, such as gliding movement, is affected by temperature.

*Arthrospira platensis*, used in the present study, is an edible filamentous cyanobacterium utilized as raw material for food and food additives [3,4]. Its products are usually commercialized under the name spirulina since this cyanobacterium was formerly classified in the genus *Spirulina*. A distinctive feature of *Arthrospira* species is that their filaments have a helicoid morphology [5], whereas most other filamentous cyanobacteria have a straight morphology. The filaments, or trichomes, of *A. platensis* exhibit gliding motility on solid media, like many other filamentous cyanobacteria.

Many strains of *A. platensis* are maintained in culture collections in the world. We are using one of those strains, *A. platensis* NIES-39, collected from Lake Chad in Africa

in our biological experiments. The temperatures around Lake Chad vary widely, with daytime temperatures reaching 35–37 °C and night-time temperatures reaching 15–20 °C in summer [6]. To investigate how this cyanobacterium responds to varying temperatures, we examined the temperature dependence in its migration velocity. We found that the velocity remained almost constant over a wide temperature range. In contrast, straight-trichome mutants isolated from the same strain had strong temperature dependence in migration velocity, like other formerly examined cyanobacteria with straight trichomes. These results indicate the presence of a temperature compensation mechanism in the migration velocity of this cyanobacterium and that the helicoid morphology is involved in the mechanism.

## 2. Materials and Methods

### 2.1. Strains

*A. platensis* NIES-39 was obtained from the Microbial Culture Collection at the National Institute for Environmental Studies (MCC-NIES), Tsukuba, in 2008. The three straight-trichome mutants (str-1, str-2, and str-3) were genetically independent spontaneous mutants found in the subcultures of this strain. These mutants were isolated as follows. In our laboratory, a stock culture of the strain NIES-39 propagated from a single trichome was stored frozen [7]. In addition to the stock culture, live subcultures were maintained for daily experiments by intermittently transferring a portion of the subculture into a fresh medium every 2–4 weeks. After the subculture was maintained for four years in this way, a trichome with straight morphology was found in 2012 when the trichomes were observed under a dissecting microscope. It was transferred to a fresh medium as a single trichome and propagated. Since its straight-trichome phenotype was stable among its progenies, we named it str-1 for its straight morphology [8]. The subculture in which str-1 was found was discarded when str-1 was isolated since siblings of str-1 could be present in this culture. After disposing of it, a new subculture was started from the original stock culture of the laboratory. The new subculture was maintained again by intermittently diluting it into a fresh medium every 2–4 weeks. The second straight-trichome mutant, str-2, was found in the subculture in 2016 after four years of maintenance of this subculture. Its single trichome was isolated and propagated as a pure line, and the subculture from which str-2 was obtained was discarded. A new subculture was started again from the original stock culture. The third straight-trichome mutant, str-3, was found and isolated in 2017 from this new subculture in the same way as str-1 and str-2. Since these mutants were obtained from independent subcultures, the mutagenic events that generated them were independent.

### 2.2. Media and Culture Conditions

*A. platensis* strains were cultured in the modified SOT medium prepared as described below. The SOT medium contains a high concentration of sodium bicarbonate and is suitable for culturing *Arthrospira* species [9]. In the modified SOT medium, boric acid was omitted from the SOT medium since it was shown to be unnecessary for *A. platensis* [10]. For the modified SOT medium, three kinds of stock solutions were used [11]. Each stock solution contained reagents in a combination that avoided the formation of insoluble salts (e.g., magnesium phosphate, calcium phosphate, and calcium carbonate) during storage. The three stock solutions for the modified SOT medium were as follows: (1) the basal solution containing, in 1 L, 16.8 g of NaHCO<sub>3</sub>, 0.5 g of K<sub>2</sub>HPO<sub>4</sub>, 2.5 g of NaNO<sub>3</sub>, and 1 g of K<sub>2</sub>SO<sub>4</sub>, (2) the macroelement solution containing, in 100 mL, 5 g of NaCl, 0.4 g of Na<sub>2</sub>·EDTA, 0.05 g of FeSO<sub>4</sub>·7H<sub>2</sub>O, 1 g of MgSO<sub>4</sub>·7H<sub>2</sub>O, and, 0.2 g of CaCl<sub>2</sub>·2H<sub>2</sub>O (reagents in this solution were dissolved in this order), and (3) the microelement solution containing, in 100 mL, 218 mg of MnSO<sub>4</sub>·5H<sub>2</sub>O, 22.2 mg of ZnSO<sub>4</sub>·7H<sub>2</sub>O, 7.9 mg of CuSO<sub>4</sub>·5H<sub>2</sub>O, and 2.1 mg of Na<sub>2</sub>MoO<sub>4</sub>·2H<sub>2</sub>O. These stock solutions were autoclaved at 121 °C for 15 min and stored at room temperature. The modified SOT medium was prepared by mixing 1 L of the basal solution, 20 mL of the macroelement solution, and 1 mL of the microelement solution. This medium was stored at room temperature for up to 1 month. In preparing SOT plates, the modified SOT medium was solidified with 1% gellan gum (Fujifilm Wako Chemicals,

Osaka, Japan) unless otherwise stated. When using gellan gum, it was autoclaved in deionized water separately from the mineral component of the medium, as in the case of using agar in cyanobacterial culture [12,13]. Light and temperature conditions were as previously described unless otherwise stated [8]. Experiments in this study were performed between the second and tenth hours of the 12 h light period unless otherwise stated.

### 2.3. Photographs and Time-Lapse Movies

Dark-field microscopic photographs were taken using the digital camera WRAYCAM-EL310 (Wraymer, Osaka, Japan) connected to the dissecting microscope S9D (Leica Microsystems, Tokyo, Japan) or the inverted microscope CKX41 (Olympus, Tokyo, Japan). Dark-field images were obtained by illuminating the microscopic samples horizontally from one side with a light source LED-W (Kyowa Optical, Sagami-hara, Japan) in a dark room. When making time-lapse movies, time-lapse images were taken by the dissecting microscope S9D equipped with an objective lens 2.0× (Cat. No.10450821, Leica Microsystems) connected with the digital camera WRAYCAM-EL310, using the function of the software Microstudio (Wraymer, Osaka, Japan), which was supplied with the digital camera. The obtained images were assembled using QuickTime Player 7 (Apple Japan, Tokyo, Japan) to make time-lapse movies. Bright-field microscopic images of trichome fragments were taken using the All-in-One Microscope BZ-9000 (Keyence, Osaka, Japan). The Rotterman Contrast illumination to visualize the trajectories of trichomes was performed using the transmitted light base TL3000 Ergo (Leica Microsystems), and microscopic images were obtained with the dissecting microscope S9D connected with the digital camera WRAYCAM-CIX2000 (Wraymer).

### 2.4. Determination of the Velocity and Trichome Lengths

*A. platensis* trichomes were placed on SOT plates (9 cm diameter) using a micropipette. The plate with the trichomes was put in a stage-top incubator (C150A; Blast Co., Kawasaki, Japan). The stage-top incubator used in this experiment was an acrylic chamber equipped with a transparent glass heater and its controller. We set the glass heater at the top of the acrylic chamber. Also, a heat insulation material made of polystyrene foam was put around the plate. Since this incubator was equipped with dual temperature sensors that could measure the temperatures of the glass heater and the internal atmosphere, we could keep the temperature around the sample at fixed temperatures. After placing the plate with *A. platensis* trichomes in this incubator, they were put on the stage of the Free-angle Observation System VHX-S90B (Keyence, Osaka, Japan) and left for 1 h for the temperature to equilibrate. Movement of the trichomes was observed from the top of the chamber using a digital microscope VHX-2000 (Keyence) equipped with a long-distance zoom lens VH-Z50L (Keyence). During the microscopic observation, the samples were illuminated from the top by the Free-angle Observation System VHX-S90B light source, which was equipped with a halogen lamp (JCR12V100W10H; Iwasaki Electric Co., Tokyo, Japan). The photosynthetic photon flux in the samples was 830  $\mu\text{mol}/\text{m}^2/\text{s}$ . In determining the velocity, the migration distance was determined using the measurement function of the digital microscope, and the velocity was calculated by dividing the migration distance by the measurement time. The lengths of the trichomes on the solid medium were determined using either the two-point measurement function or the multiple-point measurement function of the digital microscope VHX-2000, depending on the shapes of the trichomes.

### 2.5. Fragmentation of Trichomes with Ultrasound

*A. platensis* trichomes from 20 mL of the culture in the modified SOT medium were recovered on the nylon sieve with 20  $\mu\text{m}$  openings [8]. Then, they were suspended in 2 mL of fresh medium and sonicated at 25 °C for 5 s with the sonicator (Type 5202 PZT; Ohtake Works Co., Tokyo, Japan) equipped with a microtip probe. The output of the sonicator was set at 10W during sonication. The survival rate after this treatment was 31%, as determined by a colorimetric viability assay [14] (this value may be helpful when reproducing this

experiment using other models of sonicators). Trichome fragments were recovered by centrifugation at  $4000 \times g$  for 5 min at  $25\text{ }^{\circ}\text{C}$  and washed with 2 mL of the medium. Then, they were cultured for 3 days in 30 mL of the medium under standard culture conditions. Since the generation time of *A. platensis* under our culture conditions was approximately 24 h, the number of cells increased up to 8 times after 3 days, resulting in the elongation of the fragmented trichomes.

### 2.6. Statistical Analysis

All statistical analyses were performed using GraphPad Prism 8 (GraphPad Software, San Diego, CA, USA). The Kruskal–Wallis test was used to analyze the data, followed by Mann–Whitney unpaired tests. Spearman’s correlation coefficient ( $R_s$ ) was determined for evaluating the correlation of the trichome length and the migration velocity.

## 3. Results

### 3.1. Effect of Trichome Length on the Migration Velocity

The trichomes of *A. platensis* NIES-39 are helicoid in liquid media. However, when they were placed and cultured on a solid medium, they were flattened on the surface of the medium due to gravity. On the solid media, they take two distinct shapes: spiral and wavy shapes (Figure 1) [15]. Trichomes in both shapes performed uninterrupted gliding movement on the medium. The trichomes in spiral shapes rotated at almost the same places and barely changed their locations (Figure 1A, Video S1). In contrast, those in wavy shapes migrated along their longitudinal axes (Figure 1B, Video S2). We analyzed the velocity of the trichomes in wavy shapes to examine the migration speed. The velocity was determined by measuring the migration distance that the body of the cyanobacterium moved along the longitudinal axis during unit time (Figure 1B).

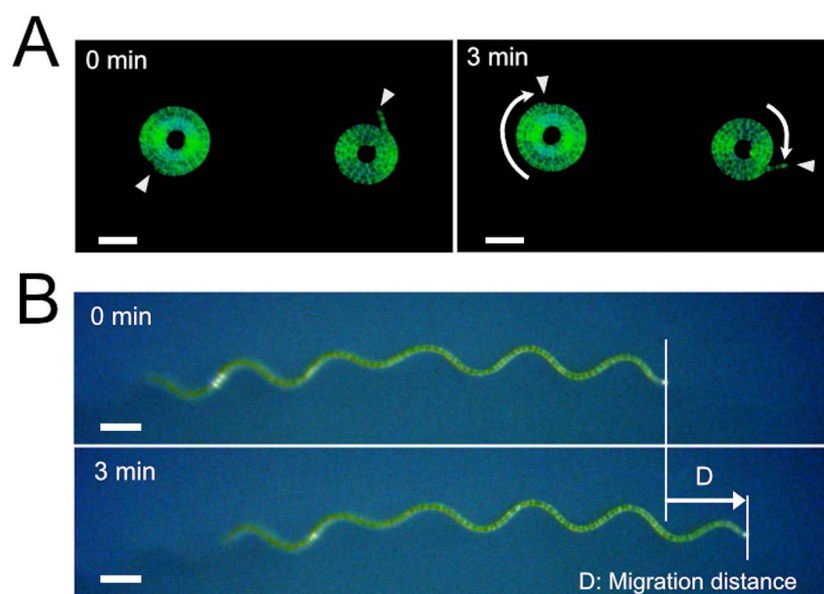


**Figure 1.** Gliding movement of *A. platensis* NIES-39 on solid medium. (A) Rotation of trichomes in spiral shape. Arrowheads show the trichome termini visible outside the spirals. Scale bars represent  $100\text{ }\mu\text{m}$ . (B) Migration of a trichome in a wavy shape. Scale bars represent  $50\text{ }\mu\text{m}$ .

Preliminary analysis performed at  $30\text{ }^{\circ}\text{C}$  suggested that the migration speed was not constant even under constant temperature and varied considerably from filament to filament. Also, there appeared to be a tendency for extremely short trichomes to exhibit slow migration speed. Most *A. platensis* NIES-39 trichomes are longer than  $200\text{ }\mu\text{m}$ , but shorter ones also exist [8]. Therefore, we first determined the effect of trichome length on the migration speed quantitatively under constant temperature at  $30\text{ }^{\circ}\text{C}$ .

Figure 2 shows the relationship between the trichome length and the migration velocity. As shown in this figure, there appeared to be a tendency for shorter trichomes to be slower than longer ones. Statistical analysis indicated a positive correlation between the length of trichomes and the migration speed (Spearman correlation coefficient  $R_s = 0.77$ ,  $p < 0.0001$ ). However, when only the data of  $\geq 250$   $\mu\text{m}$  long trichomes were used, the correlation was insignificant ( $R_s = 0.14$ ,  $p = 0.43$ ). This result indicated that the effect of trichome lengths could be mostly excluded when the data of unusually short trichomes were excluded from the analysis.

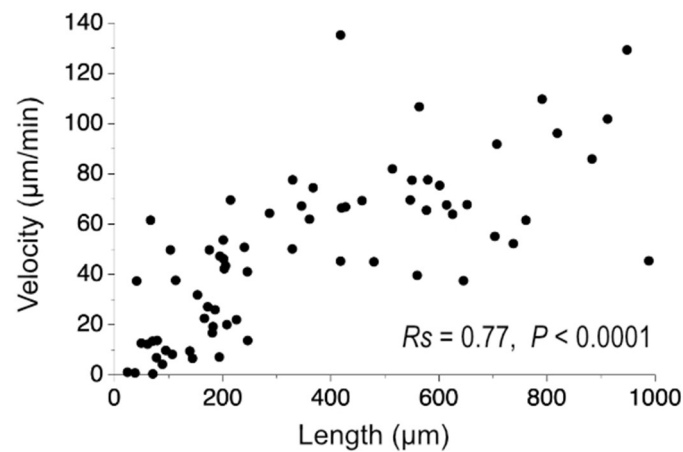


**Figure 2.** Relationship between the length along the longitudinal axis and the velocity of *A. platensis* NIES-39 trichomes. Spearman correlation coefficient ( $R_s$ ) and the  $p$ -value ( $P$ ) are shown on the panel ( $n = 70$ ).

### 3.2. Effect of Temperature on the Migration Speed of Wild-Type *A. platensis*

We next examined the effect of temperature on the longitudinal velocity of *A. platensis* NIES-39. Trichomes that were  $\geq 250$   $\mu\text{m}$  long were used in this experiment to avoid the effect of short trichomes. The result is shown in Figure 3. Although the migration velocities were variable at each temperature, it increased significantly between 20 °C and 25 °C. Also, significant increases in the migration speed with increasing temperatures were detected at 27–32 °C. In contrast to these temperatures, there was no significant change in the migration speed between 32 °C and 40 °C. The speed slowed or impaired at temperatures above 42 °C.

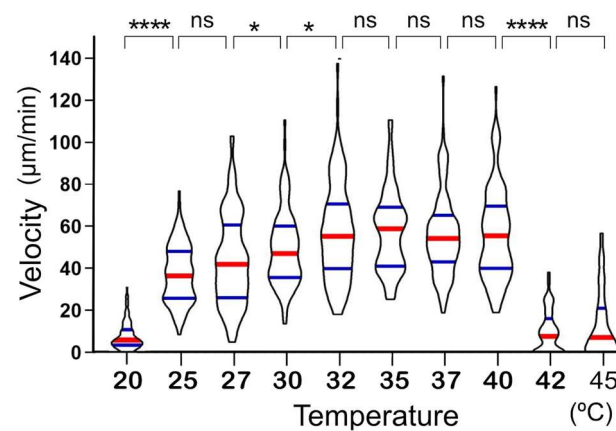


**Figure 3.** Effect of temperature on the migration velocity of the wild-type *A. platensis* NIES-39. The violin plot visualizes the data distribution for each temperature ( $n = 100$ ). The medians and quartiles are shown by the red and blue horizontal lines, respectively. Results of Mann–Whitney tests between the adjacent temperature samples are shown above the violin plots (\*,  $p \leq 0.05$ ; \*\*\*\*,  $p \leq 0.0001$ ; ns,  $p > 0.05$  (not significant)).

The pattern of the temperature-dependent change in the velocity of *A. platensis* NIES-39 was different from that in the former reports that employed cyanobacterial species with straight trichomes, in which the migration velocity increased with increasing temperatures until extremely high temperatures impaired the movement [2]. Therefore, we next examined the velocity using straight-trichome mutants of *A. platensis* NIES-39 to examine whether the shape of the trichomes affected the temperature-dependency of the migration speed.

### 3.3. Effect of Temperature on the Migration Velocity of Straight-Trichome Mutants

We used three spontaneous straight-trichome mutants (str-1, str-2, and str-3), which had been isolated from *A. platensis* NIES-39 (Figure 4). These mutants were genetically independent of each other because they were isolated in different years from independent subcultures of *A. platensis* NIES-39.

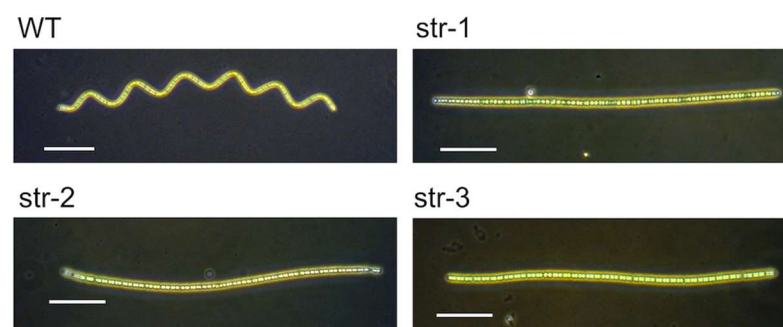


**Figure 4.** *A. platensis* NIES-39 and straight-trichome mutants. Trichomes of wild-type *A. platensis* NIES-39 (WT) and three mutants (str-1, str-2, and str-3) are shown. Scale bars represent 100  $\mu\text{m}$ .

The migration velocities of these mutants were determined under various temperatures. In this experiment, short trichomes (<250  $\mu\text{m}$ ) were excluded from the analysis, as in the case of the wild-type strain. As shown in Figure 5, consistent results were obtained with all three mutants. The velocities increased with increasing temperatures at 32–37  $^{\circ}\text{C}$ . The speed slowed down or was impaired above 40  $^{\circ}\text{C}$ .

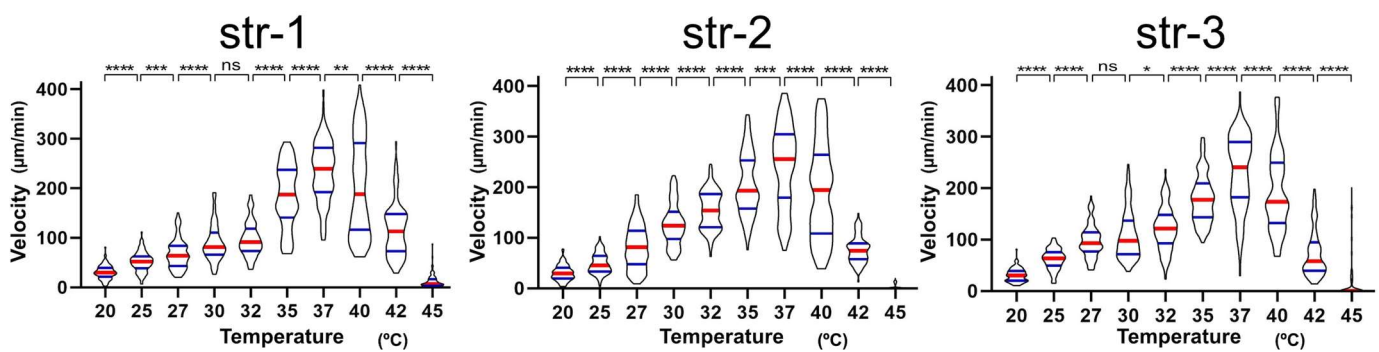


**Figure 5.** Effect of temperature on the migration velocity of straight-trichome mutants. The violin plot visualizes the data distribution for each temperature ( $n = 100$ ). The medians and quartiles are shown by the red and blue horizontal lines, respectively. Results of Mann–Whitney tests between the adjacent temperature samples are shown above the violin plots (\*,  $p \leq 0.05$ ; \*\*,  $p \leq 0.01$ ; \*\*\*,  $p \leq 0.001$ ; \*\*\*\*,  $p \leq 0.0001$ ; ns,  $p > 0.05$  (not significant)).

### 3.4. Comparison of the Temperature Dependency in the Movement of the Wild-Type Strain and the Straight-Trichome Mutants

As shown in Figure 3, the median velocities of the wild-type trichome were within the range of 40  $\mu\text{m}/\text{min}$  to 60  $\mu\text{m}/\text{min}$  in the temperature range of 27–40  $^{\circ}\text{C}$ , and no significant change was observed between 32  $^{\circ}\text{C}$  and 40  $^{\circ}\text{C}$ . In contrast, the straight-trichome mutants

showed an increase in velocity with increasing temperature up to 37 °C, with the median velocity exceeding 230  $\mu\text{m}/\text{min}$  at 37 °C (Figure 5). Since the Y-axis scales in Figures 3 and 5 differed, the mean velocities of the wild-type strain and the straight mutants are plotted on a unified Y-axis scale in Figure 6 for comparison. It is clear from this figure that the overall migration velocity of the wild-type strain is suppressed compared to that of the straight-trichome mutants. In addition, a large difference in the migration speed of the wild-type strain was not observed between 32 °C and 40 °C. It maintained similar velocities in this temperature range. In contrast, the velocity of the straight mutants increased drastically with increasing temperature between 32 °C and 37 °C. Also, between 25 °C and 32 °C, the slope of the curve is steeper in the mutants than in the wild type.

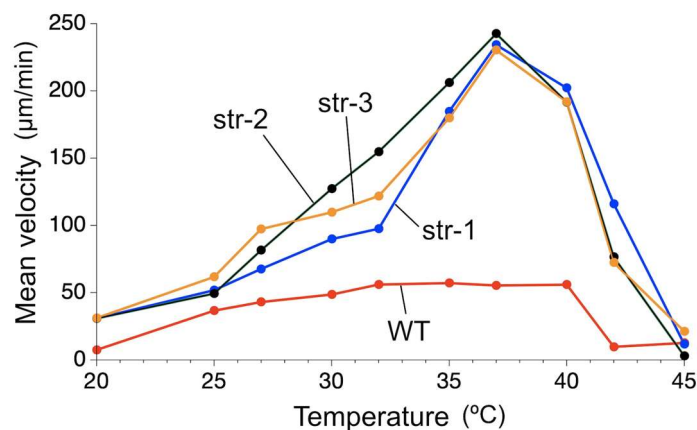


**Figure 6.** Summary of the effect of temperature on the migration velocity. The means of the data for wild-type (WT) and straight-trichome mutants (str-1, str-2, and str-3) in Figures 3 and 5 are plotted.

The three straight mutants showed a large increase in migration speed with increasing temperatures from 25 °C to 37 °C, while the wild-type strain did not show such an increase. This result indicated the existence of a mechanism that kept the migration velocity of the wild-type strain almost constant in a wide temperature range, and it is lost in the straight-trichome mutants.

### 3.5. Different Behaviors of the Wild-Type *A. platensis* and the Straight-Trichome Mutants on Solid Media

The experiments with the straight-trichome mutants demonstrated that they helped analyze the behavioral traits associated with the helicoid morphology. In the following experiments, we examined them further.

Helicoid and mutant trichomes moved considerably differently when placed on solid media. In Figure 7, the trajectories of the wild-type trichomes and the straight-trichome mutants (str-1, str-2, and str-3) were visualized by Leica Rotterman Contrast illumination that emphasized the concavity generated by the movement of trichomes. In the lower part of Figure 7A, a mostly flat, concave depression can be seen. This area was created by the accumulation of many tracks generated by the trichomes. Some trichomes left that region, leaving wavy tracks, but they quickly turned around and did not travel far. These tracks show that the wild-type trichomes mostly moved around their original positions. Figure 7B also shows the trajectory of a wild-type trichome. In this instance, the shape of the trajectory indicates that a trichome in a wavy shape moved for a while and then coiled to rotate in a spiral shape, making a round concave on the surface of the medium. Then, it uncoiled to migrate in a wavy shape. It repeated these shape changes intermittently.

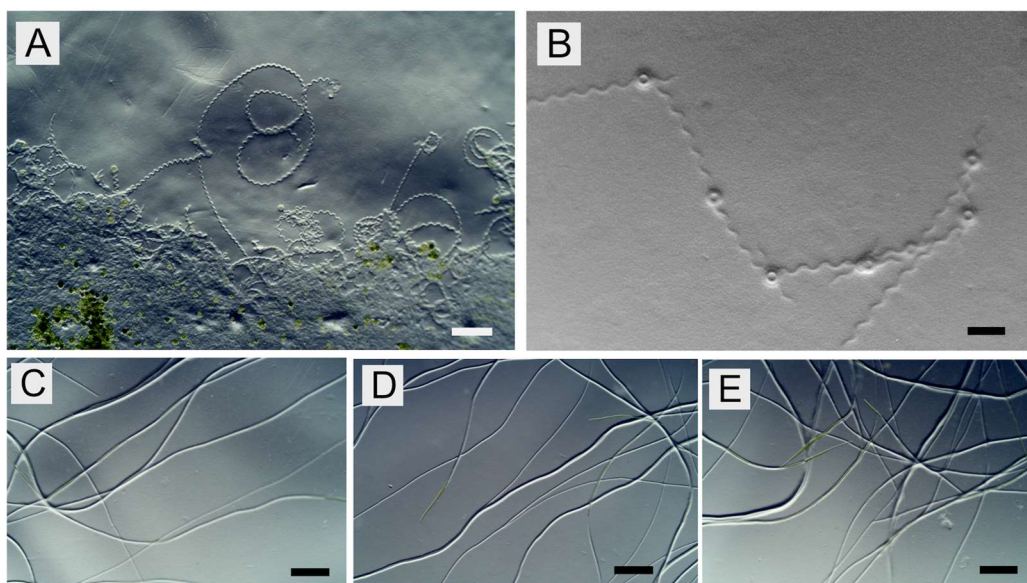


**Figure 7.** Trajectories of trichomes on solid media. The wild-type *A. platensis* NIES-39 (A,B), str-1 (C), str-2 (D), and str-3 (E) were cultured on solid media, and the concavity generated by the movement of trichomes were visualized by Leica Rotterman Contrast illumination. Scale bars in (A,C–E) represent 1 mm and that in (B) represents 200  $\mu\text{m}$ .

In contrast to the wild-type strain, straight mutants mainly moved in a particular direction, traveling a relatively long distance, although they may eventually turn gently (Figure 7C–E). The trichomes of straight mutants tended to move side-by-side when they encountered each other during the movement in the same direction. Therefore, many tracks of the straight mutants were broader than those of the wild-type strain since those tracks were formed by multiple trichomes that moved side-by-side.

In the next experiment, shown in Figure 8A, we examined the differences in the distribution of trichomes after placing them at the center of solid media (area 1 in Figure 8A). After 6 h of incubation at 30 °C, trichomes were observed under a dissecting microscope to record the number of trichomes in each area. As shown in the bar graphs in Figure 8A, 96% of wild-type trichomes remained within area 1 after 6 h. In contrast, only 11.5% of straight trichomes remained there, and 48.5% had migrated to the outermost area. This experiment demonstrated that the expansion of growth territory is suppressed in wild-type trichomes compared to that in the straight mutant.

The difference became visually evident when these strains were cultured for an extended period. The images in the left panels of Figure 8B are the wild-type *A. platensis* and the str-1 mutant on solid media after a month of cultivation. In the beginning, they were placed at the center of the media. After a month, most wild-type trichomes remained in the central area, whereas the straight mutants expanded their territory, growing in the whole area of the plate. When the trichomes of the straight mutant reached the peripheral region, many climbed the side wall of the plastic plate. Chlorosis is evident among the trichomes near the top of the side wall (“Side wall (str-1)” in Figure 8B). On the back of the lid of this plate, dry remnants of trichomes can be seen, indicating that trichomes reached even there (“Back of the lid (str-1)” in Figure 8B). We transferred these remnants to a fresh medium, but viable cells were not recovered, indicating that they were dead.

The results in Figures 7 and 8 show that wild-type *A. platensis* trichomes tend to stay around the original positions and that the helicoid morphology confers this trait. This trait suppresses the expansion of the growth territory, but at the same time, it reduces the chance of the trichomes moving to harsher environments. The temperature compensation of the migration velocity appears to be acquired as a part of such a suppression.

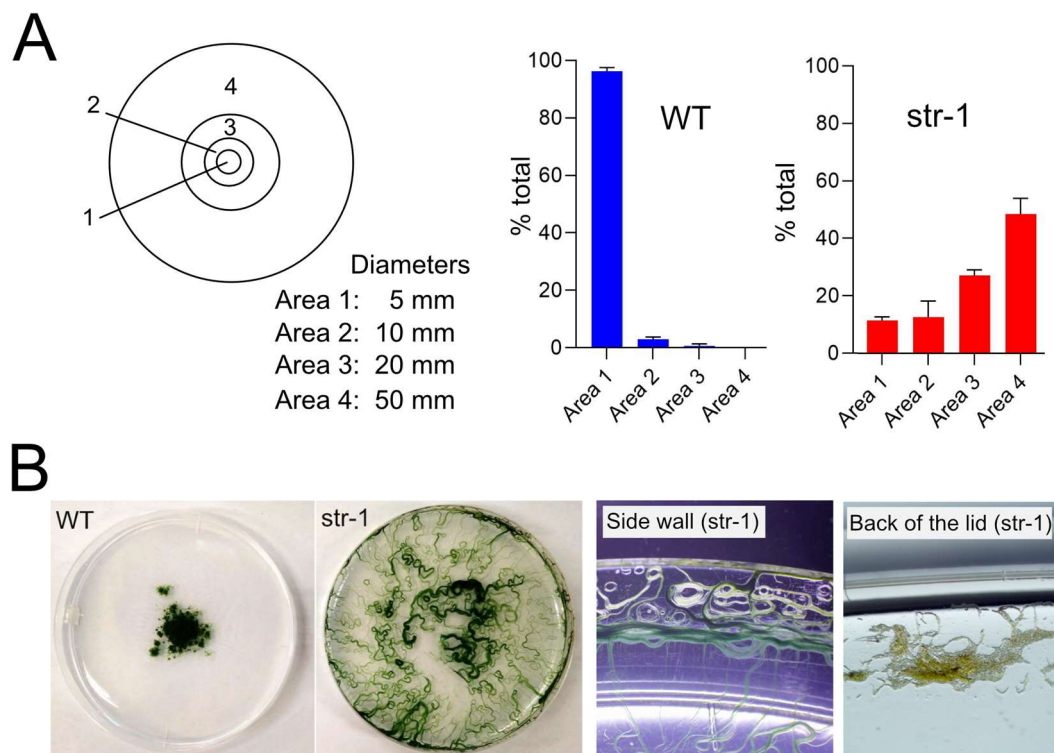


**Figure 8.** Difference in the expansion of growth territory. **(A)** Analysis of the distribution of trichomes. Trichomes were placed at the center (area 1) of solid media and incubated at 30 °C. After 6 h, the number of trichomes in each area was recorded. The experiment was repeated five times using 108–204 trichomes for each experiment, and the means and the standard deviations of % total were calculated. Results are summarized in the bar graphs. **(B)** Results of prolonged culture on solid media. The wild-type (WT) and the straight mutant (str-1) were cultured on solid media, and the photographs were taken after a month.

### 3.6. Migration Velocity of Fragmented Trichomes

In the experiment in Figure 2 that examined the relationship between the trichome length and the migration velocity, we used naturally occurring trichomes of various lengths obtained from cultures. Short trichomes tended to be slow in their migration speed in this experiment. We performed an additional experiment to clarify the reason for this phenomenon. One possible reason for the slow speed was that short trichomes were formed during unusual events in the life cycle of *A. platensis* that generated unhealthy short trichomes. If this was the case, their low speed did not necessarily reflect the nature of the gliding motility, but it might reflect the physiological state of the short trichomes. However, it is also possible that the cooperation of a high number of cells is necessary for the efficient gliding movement of trichomes. If this was the case, the slow speed of the short trichomes was because the number of cells that constituted them was too small to perform efficient movement. We examined the migration velocity of short trichomes artificially fragmented by ultrasound to differentiate between these possibilities. Cells in the short trichomes generated this way would be similar in their physiological state.

Trichomes of the wild-type strain (NIES-39) and a straight mutant (str-1) were treated mildly with ultrasound to generate fragments of the trichomes (Figure 9A). The fragmented trichomes were cultured for 3 days. Then, migration speeds along the longitudinal axis were determined at 30 °C using trichomes less than 200 µm in length. As shown in Figure 7B, trichome length was positively correlated with the migration speed both for the wild-type strain ( $R_s = 0.70$ ,  $p < 0.0001$ ) and for the straight mutant ( $R_s = 0.79$ ,  $p < 0.0001$ ). These results indicated that the physical length of the trichomes, rather than their physiological state,

affected their migration speed. Therefore, it was most likely that the cooperation of the cells constituting trichomes was involved in the efficient migration of the trichomes.

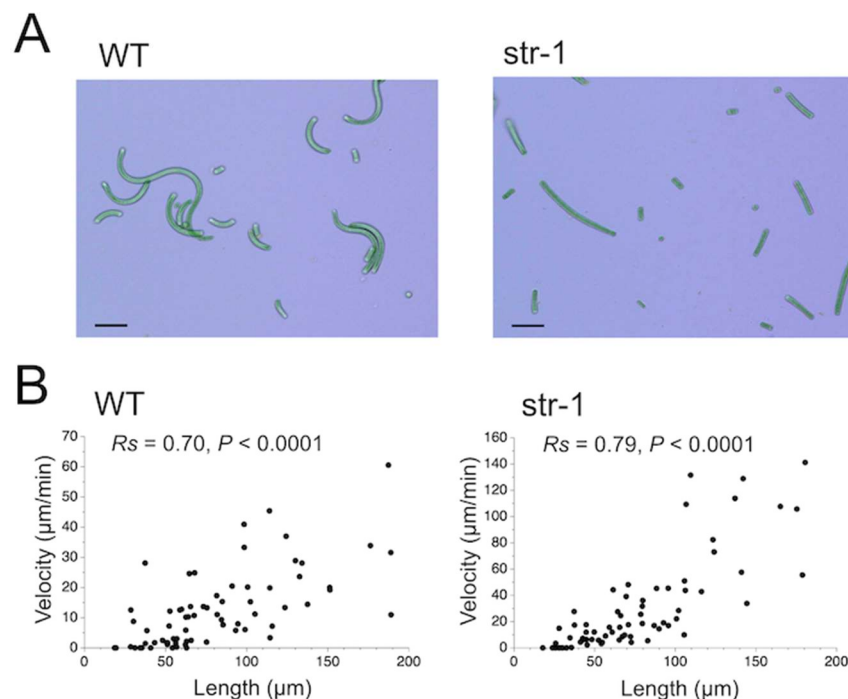


**Figure 9.** Migration velocity of short trichomes. (A) Trichome fragments of wild-type *A. platensis* NIES-39 (WT) and a straight-trichome mutant (*str-1*) after the ultrasound treatment. Scale bars represent 40 µm. (B) Relationships between the length along the axis and the migration velocity of wild-type *A. platensis* NIES-39 (WT) and a mutant (*str-1*). The length and the velocity were determined three days after the ultrasound treatment. Spearman correlation coefficient ( $R_s$ ) and the  $p$ -value ( $P$ ) are shown on each panel ( $n = 70$ ).

The velocity of the wild-type trichome fragments was relatively slower than the fragments of the straight mutant in this experiment (notice that the Y-axes are differently scaled in the graphs in Figure 9B). This difference in velocity was most likely caused by the curvature of the wild-type filaments since the direction of the propulsive force generated by the wild-type filaments was, in most parts of their body, different from the orientation of the front end of the filaments.

#### 4. Discussion

It was found that the migration velocity of *A. platensis* NIES-39 was not so much affected by temperature as the formerly examined cyanobacterial species [2]. Notably, no significant difference was detected between 32 °C and 37 °C (Figure 3). However, when examined with straight-trichome mutants, they showed a strong temperature dependency, drastically increasing migration speed as the temperature increased in this temperature range. If only one mutant strain was examined, then the temperature-dependent change in the migration velocity could be due to another unknown mutation unrelated to the morphological change. However, all the three genetically independent straight mutants showed a strong temperature dependence in migration velocity (Figures 5 and 6), like other previously examined filamentous cyanobacteria with straight trichomes. This result indicates that the helical morphology of the wild-type strain is involved in the phenomenon that its migration rate is less affected by temperature.

The rate of physical and chemical reactions is generally affected by temperature; the higher the temperature, the higher the reaction rate. Therefore, reactions in organisms also increase in rate as the temperature increases. However, some reactions in organisms should not change their rates depending on temperature. In such cases, a temperature

compensation mechanism may evolve to ensure that the rate does not change as the temperature changes. A well-known example is the temperature compensation of the circadian clock [15–17]. The phenomenon newly discovered with *A. platensis* is also a kind of temperature compensation in which the migration speed is kept almost constant in a wide temperature range.

Temperature compensation in locomotion speed has been relatively well investigated in ectothermic animals. For example, fish change the composition of their muscle tissue to adapt to low temperatures [18,19]. In this case, temperature compensation is achieved through complex mechanisms such as changes in gene expression. In contrast, in *A. platensis*, only the helicoid structure appears responsible because the temperature compensation is lost when the morphology becomes straight.

How the helicoid morphology provides temperature compensation is unclear. It has been reported that in *A. platensis*, the pitch of the helix changes in a temperature-dependent manner, and an increase in temperature gives rise to a more tightly coiled trichome [20]. Such a change in the helix structure may be related to the temperature compensation since the alteration in the pitch of the helices may change the relative direction of the propulsive force that the cells are generating. Other physical properties of the trichome, such as its firmness or resistance against bending, might change as the temperature changes. Such a change would also affect the migration velocity. How the helicoid morphology and the physical properties of the trichomes achieve temperature compensation is a subject for further study. Since the temperature compensation in *A. platensis* appears to be achieved by a relatively simple physical mechanism, its study might provide insights into the design and control of artificial micromachines [21].

Results of the experiments in Figures 7 and 8 indicated that the expansion of the growth territory is suppressed in the wild-type strain compared to the straight-trichome mutants. The experiment in Figure 8B showed that, at least on the plate, the movement mode of wild-type *A. platensis* has some merit since it reduces the chance of migration to harsher environments. *A. platensis* NIES-39 is a strain obtained from Lake Chad, where seasonal and diurnal environmental changes are tremendous [6]. In the rainy season, the daytime temperature is 35–37 °C and the night-time temperature is 15–20 °C. The lake is surrounded by a barren area of accumulated sodium carbonate complexes called natron. In the dry season, the area of the lake gradually shrinks, leaving dry crusts of minerals behind, resulting in the expanded barren area around the lake. In such an environment, the mode of the movement of the wild-type strain might be advantageous for survival over the uncontrolled fast movement seen in the straight-trichome mutants.

It is worth mentioning that the movement mode of *A. platensis* appears to have considerable variations depending on strains since a distinctively different movement mode has been reported in another strain, *A. platensis* C005 [22]. The movement of the wild-type trichomes of this strain comprises frequent random turns and most trichomes twisting around their starting point. In this strain, the longitudinal wavy motion seen in strain NIES-39 is not reported. These differences in the movement mode would reflect the differences in the natural habitats and niches of these strains.

During this investigation, it was found that trichome length affects migration velocity (Figure 9). The experimental result suggested that the smooth gliding movement was achieved by the coordinated action of a high number of cells that make up the trichome. Filamentous cyanobacteria are thought to have evolved from unicellular cyanobacteria [23,24]. The results of our study suggest that the ability to perform efficient gliding movement was acquired only after the evolution of the body structure of the filamentous cyanobacteria, in which multiple cells are connected in tandem so that they can work cooperatively. Therefore, the potential ability to perform efficient gliding movement would have been one of the advantages that the filamentous cyanobacteria acquired when they evolved from unicellular cyanobacteria.

## 5. Conclusions

The velocity of the gliding movement of filamentous cyanobacteria with straight trichomes is affected by temperature, and generally, the higher the temperature, the faster the speed. In contrast, this study showed that *A. platensis* NIES-39 keeps a relatively constant migration velocity under various temperatures. This temperature compensation was lost in three genetically independent straight-trichome mutants isolated using *A. platensis* NIES-39 as a parental strain. These results indicate that the temperature compensation in the migration velocity of this cyanobacterium is achieved by its helicoid morphology. We also examined the effect of the trichome length on the migration velocity. Trichome length was positively correlated with the migration velocity when short trichomes were used for the analysis. This result indicates that the cooperation of a high number of cells constituting the trichome is required for the efficient gliding movement of this cyanobacterium.

**Supplementary Materials:** The following supporting information can be downloaded at: <https://www.mdpi.com/article/10.3390/phycolgy4010006/s1>, Video S1: Time-lapse movie of the gliding movement of *A. platensis* NIES-39 in spiral shapes; Video S2: Time-lapse movie of the gliding movement of *A. platensis* NIES-39 in a wavy shape.

**Author Contributions:** Conceptualization, supervision, methodology, investigation, data curation, validation, formal analysis, project administration, and writing—original draft preparation, H.S.; methodology, investigation, and formal analysis, M.S.; methodology, investigation, and formal analysis, A.S.N. All authors have read and agreed to the published version of the manuscript.

**Funding:** Research support for this study was provided through a management expense grant to Kyoto University from the Ministry of Education, Culture, Sports, Science and Technology of Japan.

**Institutional Review Board Statement:** Not applicable.

**Data Availability Statement:** Data are contained within the article.

**Conflicts of Interest:** The authors declare no conflicts of interest.

## References

1. Hoiczky, E. Gliding motility in cyanobacteria: Observations and possible explanations. *Arch. Microbiol.* **2000**, *174*, 11–17. [[CrossRef](#)] [[PubMed](#)]
2. Burkholder, P.R. Movement in the Cyanophyceae. *Quart. Rev. Biol.* **1934**, *9*, 438–459. [[CrossRef](#)]
3. Belay, A. Biology and industrial production of *Arthrospira* (*Spirulina*). In *Handbook of Microalgal Culture: Applied Phycology and Biotechnology*, 2nd ed.; Richmond, A., Hu, Q., Eds.; Wiley Blackwell: West Sussex, UK, 2013; pp. 339–358. [[CrossRef](#)]
4. Furmaniak, M.A.; Misztak, A.E.; Franczuk, M.D.; Wilmotte, A.; Waleron, M.; Waleron, K.F. Edible cyanobacterial genus *Arthrospira*: Actual state of the art in cultivation methods, genetics, and application in medicine. *Front. Microbiol.* **2017**, *8*, 2541. [[CrossRef](#)] [[PubMed](#)]
5. Castenholz, R.W.; Rippka, R.; Herdman, M.; Wilmotte, A. Form-*Arthrospira*. In *Bergey's Manual of Systematics of Archaea and Bacteria*; Trujillo, M.E., Dedysh, S., DeVos, P., Hedlund, B., Kämpfer, P., Rainey, F.A., Whitman, W.B., Eds.; John Wiley & Sons: Hoboken, NJ, USA, 2015; pp. 1–3. [[CrossRef](#)]
6. Batello, C.; Marzot, M.; Touré, A.H. *The Future Is an Ancient Lake: Traditional Knowledge, Biodiversity and Genetic Resources for Food and Agriculture in Lake Chad Basin Ecosystems*; Food and Agriculture Organization of the United Nations: Rome, Italy, 2004.
7. Shiraishi, H. Cryopreservation of the edible alkalophilic cyanobacterium *Arthrospira platensis*. *Biosci. Biotechnol. Biochem.* **2016**, *80*, 2051–2057. [[CrossRef](#)] [[PubMed](#)]
8. Shiraishi, H. Association of heterotrophic bacteria with aggregated *Arthrospira platensis* exopolysaccharides: Implications in the induction of axenic cultures. *Biosci. Biotechnol. Biochem.* **2015**, *79*, 331–341. [[CrossRef](#)] [[PubMed](#)]
9. Ogawa, T.; Terui, G.J. Studies on the growth of *Spirulina platensis*: (I) On the pure culture of *Spirulina platensis*. *Ferment. Technol.* **1970**, *48*, 361–367.
10. Tadama, S.; Shiraishi, H. Growth of the edible microalga *Arthrospira platensis* in relation to boron supply. *Int. J. GEOMATE* **2017**, *12*, 90–95. [[CrossRef](#)]
11. Shiraishi, H.; Tabuse, Y. The *ApII* restriction-modification system in an edible cyanobacterium, *Arthrospira* (*Spirulina*) *platensis* NIES-39, recognizes the nucleotide sequence 5'-CTGCAG-3'. *Biosci. Biotechnol. Biochem.* **2013**, *77*, 782–788. [[CrossRef](#)]
12. Allen, M.M. Simple conditions for growth of unicellular blue-green algae on plates. *J. Phycol.* **1968**, *4*, 1–4. [[CrossRef](#)]
13. Rippka, R. Isolation and purification of cyanobacteria. *Methods Enzymol.* **1988**, *167*, 3–27. [[CrossRef](#)]

14. Shiraiishi, H.; Toyoda, A. The use of a 3-(4,5-dimethylthiazol-2-yl)-2,5-diphenyl tetrazolium bromide-based colorimetric assay in the viability analysis of the filamentous cyanobacterium *Arthrospira platensis*. *Biosci. Biotechnol. Biochem.* **2021**, *85*, 739–742. [[CrossRef](#)]
15. Van Eykelenburg, C.; Fuchs, A. Rapid reversible macromorphological changes in *Spirulina platensis*. *Naturwissenschaften* **1980**, *67*, 200–201. [[CrossRef](#)]
16. Cai, Y.D.; Chiu, C. *Timeless* in animal circadian clocks and beyond. *FEBS J.* **2022**, *289*, 6559–6575. [[CrossRef](#)] [[PubMed](#)]
17. Patnaik, A.; Alavilli, H.; Rath, J.; Panigrahi, K.C.S.; Panigrahy, M. Variations in circadian clock organization & function: A journey from ancient to recent. *Planta* **2022**, *256*, 91. [[CrossRef](#)] [[PubMed](#)]
18. Johnson, C.H.; Egli, M. Metabolic compensation and circadian resilience in prokaryotic cyanobacteria. *Ann. Rev. Biochem.* **2014**, *83*, 221–247. [[CrossRef](#)] [[PubMed](#)]
19. Johnston, I.A.; Temple, G.K. Thermal plasticity of skeletal muscle phenotype in ectothermic vertebrates and its significance for locomotory behaviour. *J. Exp. Biol.* **2002**, *205*, 2305–2322. [[CrossRef](#)] [[PubMed](#)]
20. Van Eykelenburg, C. The ultrastructure of *Spirulina platensis* in relation to temperature and light intensity. *Antonie Leeuwenhoek* **1979**, *45*, 369–390. [[CrossRef](#)] [[PubMed](#)]
21. Huang, T.; Gu, H.; Nelson, B.J. Increasingly intelligent micromachines. *Ann. Rev. Control Robot. Auton. Syst.* **2022**, *5*, 279–310. [[CrossRef](#)]
22. Chaiyasitdhi, A.; Miphonpanyatawichok, W.; Riehle, M.O.; Phatthanakun, R.; Surareungchai, W.; Kundhikanjana, W.; Kuntanawat, P. The biomechanical role of overall-shape transformation in a primitive multicellular organism: A case study of dimorphism in the filamentous cyanobacterium *Arthrospira platensis*. *PLoS ONE* **2018**, *13*, e0196383. [[CrossRef](#)]
23. Bonner, J.T. The origins of multicellularity. *Integr. Biol.* **1998**, *1*, 27–36. [[CrossRef](#)]
24. Hammerschmidt, K.; Landan, G.; Tria, F.D.K.; Alcorta, J.; Dagan, T. The order of trait emergence in the evolution of cyanobacterial multicellularity. *Genome Biol. Evol.* **2020**, *13*, evaa249. [[CrossRef](#)] [[PubMed](#)]

**Disclaimer/Publisher’s Note:** The statements, opinions and data contained in all publications are solely those of the individual author(s) and contributor(s) and not of MDPI and/or the editor(s). MDPI and/or the editor(s) disclaim responsibility for any injury to people or property resulting from any ideas, methods, instructions or products referred to in the content.